NRIAG Journal of Astronomy and Geophysics (2014) 3, 137–149

National Research Institute of Astronomy and Geophysics

NRIAG Journal of Astronomy and Geophysics

www.elsevier.com/locate/nrjag

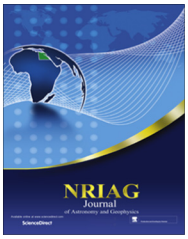

Characterization of the groundwater aquifers at El Sadat City by joint inversion of VES and TEM data

Usama Massoud [a,b], Abeer A. Kenawy [c], El-Said A. Ragab [a], Abbas M. Abbas [a], Heba M. El-Kosery [a,*]

[a] *National Research Institute of Astronomy and Geophysics, NRIAG, 11421 Helwan, Cairo, Egypt*
[b] *Department of Environment Systems, Graduate School of Frontier Sciences, Tokyo University, 5-1-5, Kashiwanoha, Kashiwa-shi, Chiba 277-8563, Japan*
[c] *Geology Department, Faculty of Science, Zagazig University, 44519 Zagazig, Egypt*

Received 14 August 2014; revised 17 September 2014; accepted 9 October 2014
Available online 4 November 2014

KEYWORDS

VES–TEM;
Joint inversion;
Groundwater exploration
El Sadat City

Abstract Vertical Electrical Sounding (VES) and Transient ElectroMagnetic (TEM) survey have been applied for characterizing the groundwater aquifers at El Sadat industrial area. El-Sadat city is one of the most important industrial cities in Egypt. It has been constructed more than three decades ago at about 80 km northwest of Cairo along the Cairo–Alexandria desert road. Groundwater is the main source of water supplies required for domestic, municipal and industrial activities in this area due to the lack of surface water sources. So, it is important to maintain this vital resource in order to sustain the development plans of this city.

In this study, VES and TEM data were identically measured at 24 stations along 3 profiles trending NE–SW with the elongation of the study area. The measuring points were arranged in a grid-like pattern with both inter-station spacing and line–line distance of about 2 km. After performing the necessary processing steps, the VES and TEM data sets were inverted individually to multi-layer models, followed by a joint inversion of both data sets. Joint inversion process has succeeded to overcome the model-equivalence problem encountered in the inversion of individual data set. Then, the joint models were used for the construction of a number of cross sections and contour maps showing the lateral and vertical distribution of the geoelectrical parameters in the subsurface medium. Interpretation of the obtained results and correlation with the available geological and hydrogeological information revealed TWO aquifer systems in the area. The shallow Pleistocene aquifer

* Corresponding author.
Peer review under responsibility of National Research Institute of Astronomy and Geophysics.

ELSEVIER Production and hosting by Elsevier

http://dx.doi.org/10.1016/j.nrjag.2014.10.001

consists of sand and gravel saturated with fresh water and exhibits large thickness exceeding 200 m. The deep Pliocene aquifer is composed of clay and sand and shows low resistivity values. The water-bearing layer of the Pleistocene aquifer and the upper surface of Pliocene aquifer are continuous and no structural features have cut this continuity through the investigated area.

1. Introduction

El Sadat city is one of the largest and important industrial cities in Egypt. It has been constructed more than 3 decades ago at about 80 km northwest of Cairo along the Cairo–Alexandria desert road. El Sadat city, and its surrounding areas, are bounded by latitudes 30° 17′ and 30° 36′ N and longitudes 30° 24′ and 30° 42′ E (Fig. 1), and accommodate a population number of 500,000 capita after the estimate of 2000. Great and continuous, governmental and popular, efforts are being paid to develop this area in the form of big agricultural and industrial projects.

El Sadat city suffers from lack of surface water supplies. Naturally, in case of shortage of surface water, one has to depend totally or partially on groundwater. Then, groundwater has been used as the main source of water in this area. Approximately, El Sadat city and the nearby villages, depend totally on the groundwater for drinking, agricultural and industrial activities. Pleistocene aquifer is the main groundwater reservoir in this area. Great attention is being paid to this aquifer due to its high water content and good quality as it is mainly recharged from the Nile Delta fresh aquifer. Northeast of El Sadat city, TWO waste water ponds (oxidation ponds) have been constructed and used for collection of domestic and industrial waste materials via a network of pipelines. Waste water contains many pollutant materials which may be penetrated down to the Pleistocene aquifer and negatively affect the water quality. Although numerous studies have been conducted in the western Nile Delta region including the El Sadat area, continuous studies are still needed for monitoring of spatial and temporal variations in the quantity and quality of the groundwater bodies and for maintaining these available water resources in order to sustain the development plans of this city.

Electrical resistivity (ER) and electromagnetic (EM) methods are well known in exploration geophysics and commonly applied in near surface applications (e.g., Christensen and Sørensen, 1998; Massoud et al., 2009; Khalil et al., 2013). ER is one of the most useful techniques applied to groundwater studies, because resistivity of a rock is very sensitive to its water saturation, and in turn, resistivity of water is very sensitive to its ionic content. Then, it is able to map different stratigraphic units in a geologic section based on their resistivity contrast. Similarly, EM techniques have been particularly succeeded in groundwater exploration and in mapping of groundwater contamination and saltwater/freshwater interfaces (e.g., Massoud et al., 2010; Khalil et al., 2013; Metwaly et al., 2014).

This study aims at characterizing the groundwater aquifers at El Sadat city, describing their spatial distribution and delineating the most suitable sites for drilling new water wells by joint inversion of VES and TEM data.

2. Geological setting

2.1. Geomorphology and stratigraphy

Several authors have addressed the geomorphology and geology of the western Nile Delta region, among them are Shata (1953, 1955), Said (1962), Attia (1975), El-Ghazawi (1982), Abdel-Baki (1983), Diab et al. (1995), Dawoud et al. (2005), El-Kashouty and Sabbagh (2011). They concluded that the western Nile Delta region comprises FOUR geomorphological units; the young alluvial plains, old alluvial plains, fanglomerates, and sand dunes. The young alluvial plains dominate the cultivated lands bordering the channel of the River Nile and its branches. These plains cover most of the Nile Delta regions and are dissected by irrigation canals and drains. They are almost flat and sloping regionally from south to north and from both sides toward the river channel. The ground elevation ranges from about 18 m above the sea level (m asl) in the south to about 4 m asl at the north with a gentle slope of about 1 m/10 km (Saleh, 1980). The old alluvial plains lie directly to the south of young alluvial plains, with an elevation ranging between 20 and 60 m. These plains expand over the western fringes of the Nile Delta and occupy most of the newly reclaimed areas. Fanglomerates represent the wadi wash brought by the drainage lines depositing their loads in shallow depressions before reaching the Nile. Traverse sand dunes are well developed on both sides of the Nile Delta as bars of loose sand, mainly directed NNW-SSE and extend for several hundred meters.

The surface of western Nile Delta region is generally occupied by sedimentary outcropping units ranging in age from Late Cretaceous to Quaternary (Fig. 2), while the subsurface stratigraphic succession comprises rock units from Triassic, Jurassic, Cretaceous, Eocene, Oligocene, Miocene, Pliocene and Quaternary ages. This extended sedimentary section constitutes a total thickness of about 4000 meters and rests unconformably over the basement complex (Abdel Baki, 1983).

El Shazly et al. (1975) used remote sensing of Landsat-1 images to classify the western Nile Delta structure. They statistically analyzed and classified the lineaments (fractures and faults) by trend into three major sets; N55°W–S55°E, N85°W–S85°E and N75°E–S75°W.

2.2. Hydrogeological setting

There are four main aquifer systems in the western Nile Delta region; the Quaternary, Pliocene, Miocene and Oligocene aquifers (Fig. 3). The *Quaternary aquifer* occupies the northern and northeastern parts of the western Nile Delta region and represents the main water-bearing layer in the area locating east of Abu Rawash–Khatatba–El Sadat–Alexandria line.

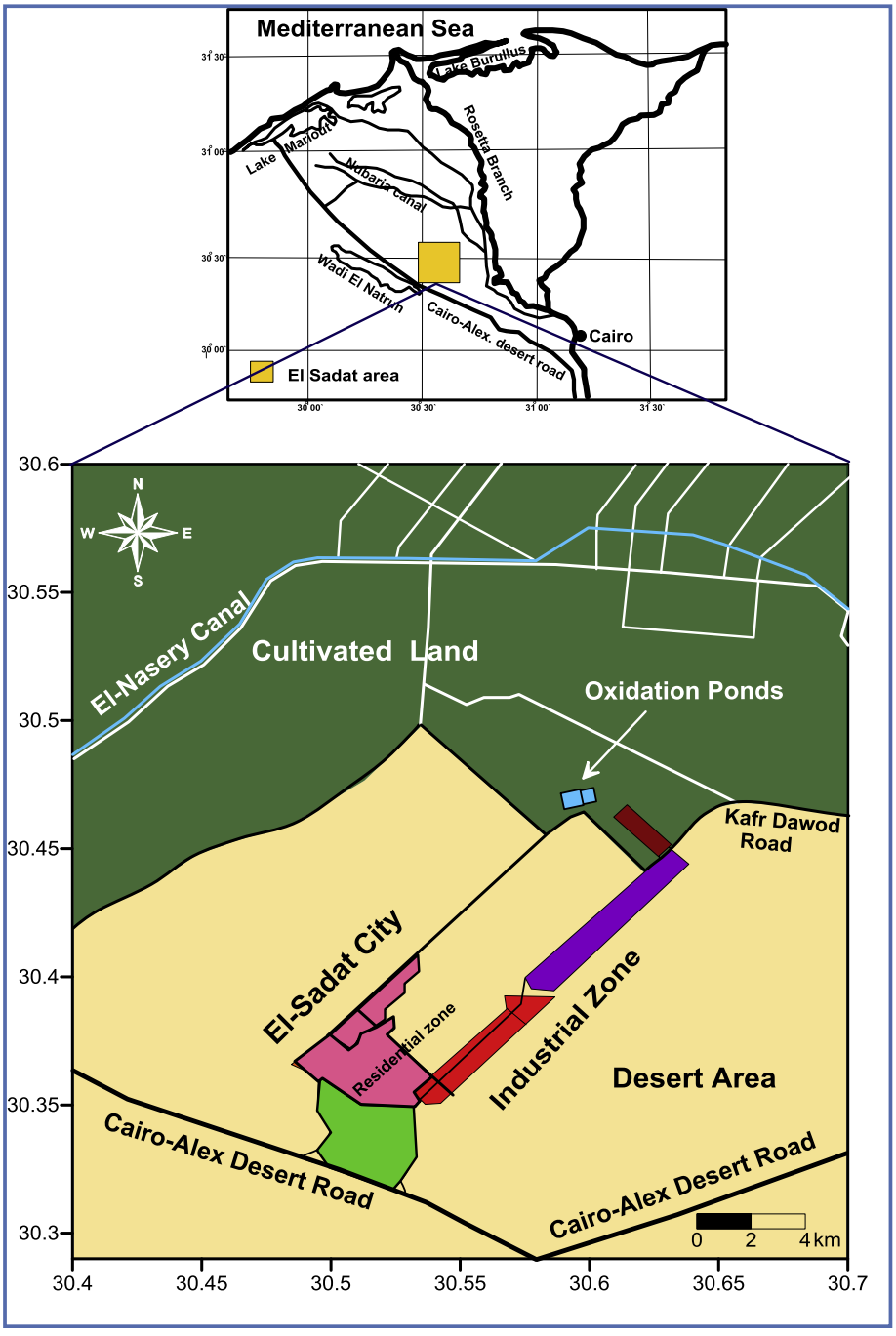

Figure 1 Location map of El Sadat city and its surroundings.

It consists mainly of successive layers of Pleistocene graded sand and gravel with some clay lenses and attains a total thickness of about 300 m near Kom Hamada to about 80 m near Wadi El Natrun. The aquifer is semi-confined in the Delta area as it is capped by a Holocene layer of sandy clay and silt with a mean thickness of 20 m, while it is unconfined at the rest of the area. The Quaternary aquifer is mainly recharged from the main Delta aquifer in addition to nearby surface canals and infiltration from excess irrigation water (RIGW and IWACO, 1990).

Wadi El Natrun aquifer is a local aquifer of the Pliocene age that consists of alternative layers of sand and clay facies and rests on the top of Moghra Formation at Wadi El Natrun depression. It is mainly recharged by lateral seepage from the Nile Delta and Moghra aquifers (Abdel Baki, 1983). The groundwater of the Pliocene aquifer varies from fresh to brackish water and the aquifer thickness is about 140 m with a saturated thickness of 90 m. The thickness decreases from east to west and also to the south of Wadi El Natrun. Miocene (Moghra) aquifer is located in the western Delta with a thickness ranging from 50 to 250 m. It covers about 50,000 km^2 and consists of Lower Miocene sand and gravel of Moghra Formation. The groundwater flow in the Moghra aquifer is generally directed westward toward Qattara Depression (Dawoud et al., 2005). It contains fresh water with salinity that increases

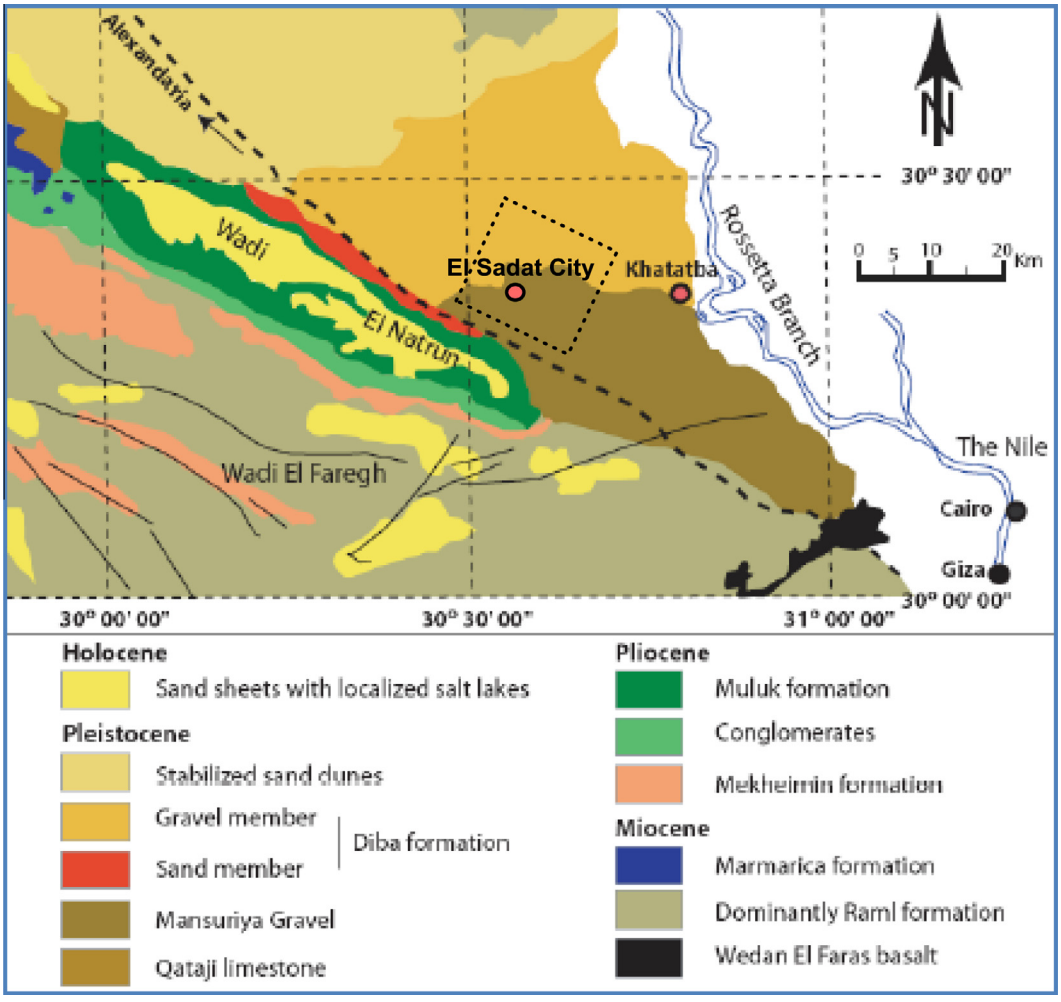

Figure 2 Geologic map of the area around El Sadat city (modified after Abu Zeid, 1984).

toward the north and west. The water quality and sustainability of this aquifer are at risk due to the rapid development of land reclamation in this area. The *Oligocene aquifer* consists of sands and gravels with clay inter beds as well as thin limestone bands at the base and thick basaltic sheet at the top. The Oligocene sediments fill the main channel of Wadi El Natrun with a total thickness of about 400 m.

2.3. Groundwater situation

Since the early eighties, the private sectors in Egypt have started to reclaim the western fringes of the Nile Delta region depending mainly on the groundwater resources. The reclamation process was accelerated during the eighties and up till now (Wassef, 2011). The total groundwater abstraction was estimated at 870 million m^3/year by the year 2000 and increased to more than one billion m^3/year in 2007 (The World Bank, 2007). The groundwater table started to decline due to the unplanned groundwater abstraction, and over pumping from production wells while the aquifers receive little or no replenishment particularly during the last decades because of the scarcity in the rainfalls (Ghaly, 2001).

2.4. El Sadat City

El Sadat city and its surrounding area belong to the old alluvial plains, which dominate the newly reclaimed lands west of Rosetta branch, with low to moderate elevations ranging from 20 to 60 m asl. The northeastern part of the study area is occupied by cultivations and agricultural activities, while the southwestern part is a desert land with some building activities and local farms. The ground surface in the study area is smooth and the elevation does not exceed 50 m asl with a gentle slope from south to north. No depressions, hills or major surface features are identified in the study area. The area is covered by Quaternary clastics composed mainly of sand and gravel with some clay pockets. Pleistocene aquifer is the main source of water in the El Sadat area and almost all the productive wells in the El Sadat area tap this aquifer, while Pliocene and Miocene aquifers dominate at Wadi El Natrun (southwest). Pleistocene aquifer is a widely distributed aquifer extended from Rosetta branch (east) to Wadi El Natrun (west). It is composed of thick sections of successive layers of graded sand and gravel with clay lenses as shown in Fig. 4. This aquifer is mainly recharged from the Nile Delta aquifer in addition to the surface canals of El-Rayah El-Beheiry, El-Rayah El-Nasery and El Nubariya

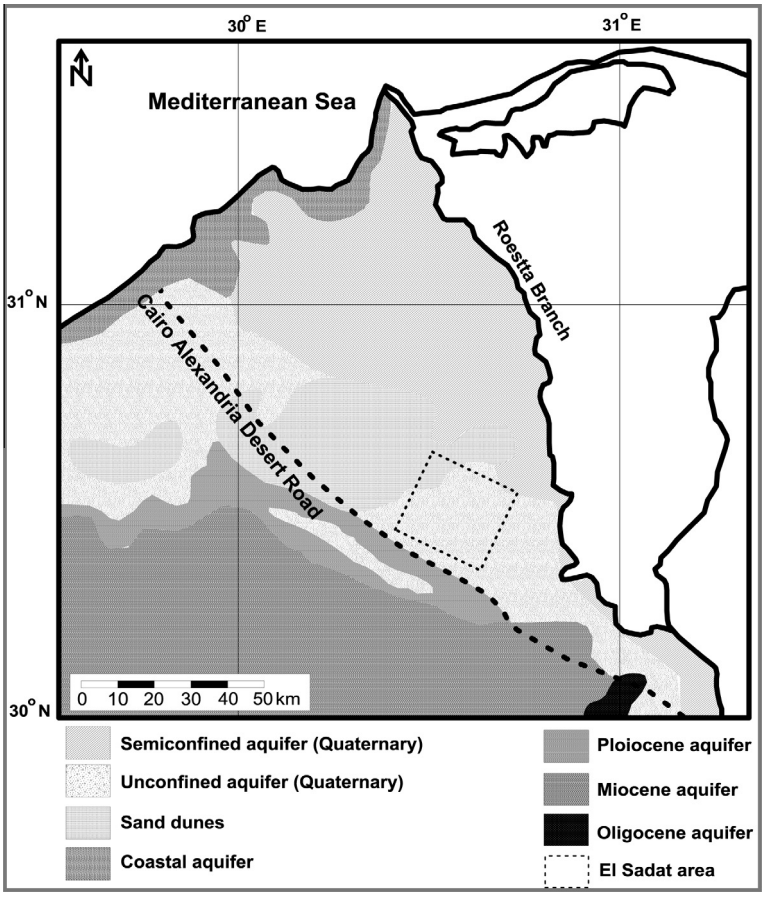

Figure 3 Groundwater aquifers in the western Nile Delta (modified, RIGW and IWACO, 1991).

canal. Minor feeding also comes from rainfall and infiltration from excess irrigation water.

As a part of the semi-arid zone, the area is characterized by a long hot summer and a short warm winter, low rainfall and high evaporation. Although different groundwater aquifers are available and can be used for water supplies in the El Sadat area, it is suffering from water supply shortage, groundwater depletion and quality deterioration due to the unmanaged over-exploitation of this water resource. This is because this city depends mainly on the groundwater in its industrial, agricultural and domestic activities. Besides, the aquifers have no replenishment due to the limited rainfalls and little recharge from the green areas which was estimated at 0.5 mm/day (RIGW, 2002). Accordingly, continuous studies are necessary for evaluation, monitoring and management of this vital water resource in this area.

3. Data acquisition

In the present study, VES and TEM data were measured at 24 stations in the study area, where the two data sets were measured at the same locations to be suitable for the joint inversion process. The study area which was covered by the geophysical survey is bounded by latitudes 30°21′ and 30° 33′ N and longitudes 30° 30′ and 30° 42′ E as shown in Fig. 5. The measuring points were arranged along 3 profiles trending NE–SW coincide with the elongated side of the study area, where the inter-stations spacing and the line-to-line separation are around 2 km. The measuring points were close to some water wells dug by individuals, where some information (e.g. well depth, depth of water, screen depth, water quality. . .etc.) could be obtained and used as assistant means in the interpretation process. Resistivity data have been measured by *SYSACAL R2* resistivity meter, where the standard Schlumberger-electrode array with current electrode (AB) spacing varies logarithmically from 2 to 1000 m. The TEM data were measured by *SIROTEM MK3* instrument at 23 stations in the study area. The location of VES No. 6 was excluded from TEM data recording due to the limited open area at this site. At some stations, the TEM recording was repeated 2–3 times with different acquisition parameters and the record with highest signal/noise ratio was selected for analysis. The common single-squared loop configuration with a side length of 50 m has been used in this work.

4. Data analysis

4.1. Individual inversions

Before the joint inversion process, the VES and TEM sounding curves were qualitatively investigated to show the lateral and vertical behaviors in the electrical properties dominating in the study area. This was followed by an individual inversion of the VES and TEM data. The VES data were inverted by the computer-based program, IPI2Win-1D (2000), which is designed for automated and interactive semi-automated interpretation of VES data. Inversion of the TEM data was

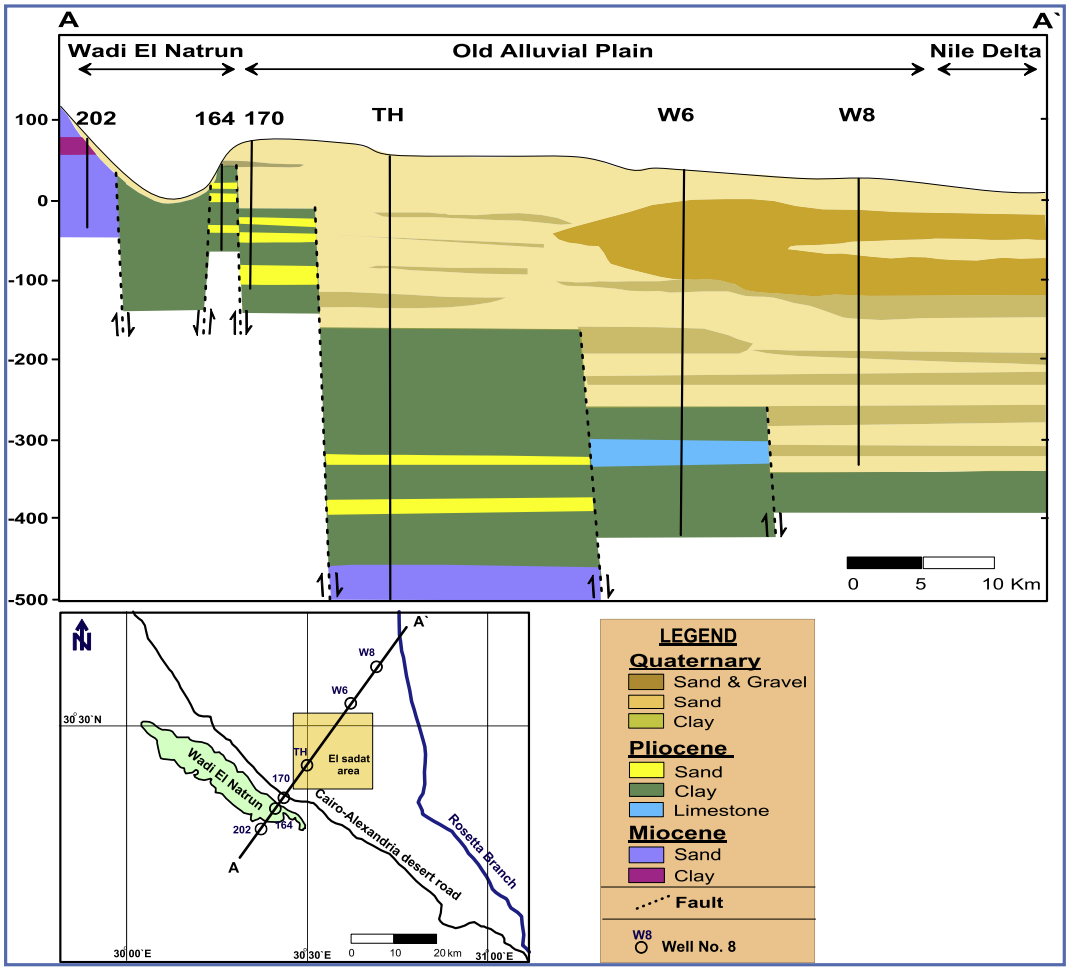

Figure 4 Geological/hydrogeological cross-section of the shallow aquifers between Rosetta branch and Wadi El Natrun (modified, El-Abd, 2005).

conducted using the TEMIX XL 4 (1996) software. Fig. 6 shows some examples of the multi-layer models obtained from the VES and TEM data inversions.

In this work, we have used the individual inversions of the VES and TEM data sets just for comparison between their results, to reveal the points of similarity and discrepancy between them and to show the necessity of the joint inversion process. To achieve this concept, the VES models were used for the construction of three cross sections along the lines A–A′, B–B′ and C–C′ as shown in Fig. 5. Similarly, three TEM cross sections were constructed along the same lines.

Then, correlation between the comparable sections [section A from VES with section A from TEM], [B (VES)–B (TEM)] and [C (VES)–C (TEM)], revealed that both the VES and TEM techniques provide a similar trend of sounding curves with some variations in the resistivity values. Besides, the VES sections produced SIX layers, while the TEM sections show FOUR layers although they have reached approximately to the same depth. These differences are significant and accepted when understood in the light of the operation principle of each technique as clarified below.

- In DC resistivity, the electric current lines intersect a number of interfaces before giving rise to the measured voltage. Then, the measured resistivity values (p_a) are almost a volumetric resistivity average of a layer set defined by the current pathways and the used array. In contrast to the TEM soundings, the current lines in the ground are images of the transmitter loop. The current filament moves outward and downward like smoke rings. Accordingly, the receiver response is affected by the vertical, as well as, the lateral variation in the resistivity values.
- The sensed volume of the ground is different. In the DC sounding, a large volume of the ground contributes in the measured response, while the ground volume in TEM sounding is limited by, or slightly wider than, the loop area.
- The DC resistivity is more sensitive and can distinguish the near surface medium into thin layers. However, the TEM method is sensitive in deep medium and cannot differentiate the shallow section into thin sheets, but rather, compile the uppermost 10–15 m into one layer.
- DC resistivity is sensitive to resistive medium, while the TEM method is sensitive to the conductive medium as the induction process is strong in low resistivity medium.

Due to the different behaviors and selective sensitivities of the VES and TEM soundings, we can maximize the benefit by joining the two data sets in one optimization process to obtain one multi-layer model at each station that satisfies both data sets, the so called "joint inversion".

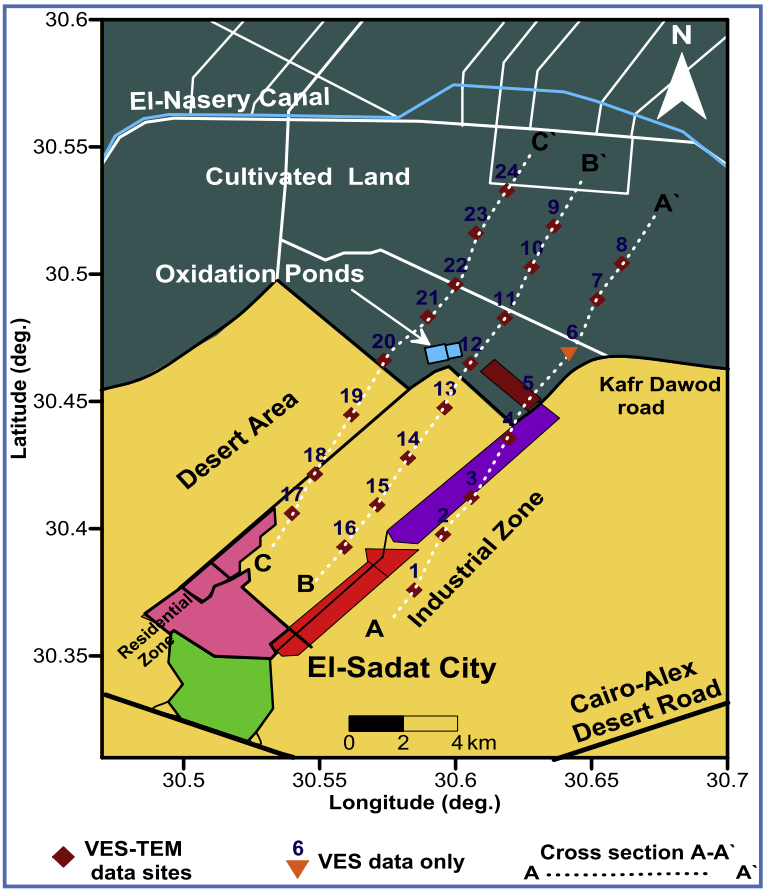

Figure 5 Location of VES–TEM stations and geoelectrical cross sections at the study area.

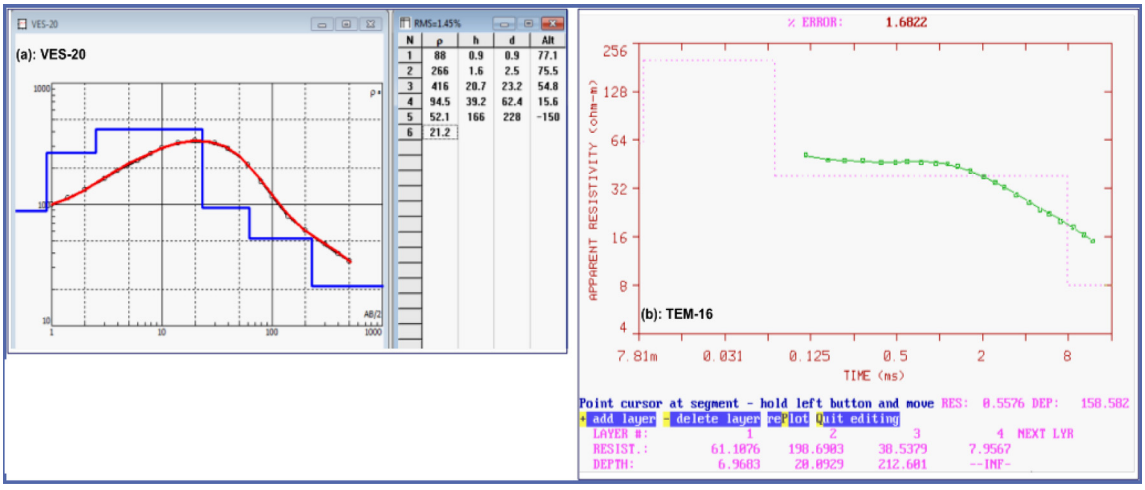

Figure 6 The models obtained from the VES and TEM data inversion at (a): VES No. 20 and (b): TEM No. 16.

4.2. Joint inversion

Numerous studies have shown that, the joint inversion of galvanic and inductive data, where a single model satisfies both data sets, will enhance the resolution of subsurface resistivity structure (Jupp and Vozoff, 1975; Raiche et al., 1985; Sandberg, 1993; Massoud et al., 2009; Khalil et al., 2013). Thus, the inclusion of TEM data in the VES data set can: (1) reduce problems with layer suppression and (2) reduce the low and high resistivity equivalences that may be encountered using only a single method. This cooperative process generally implies that two related data sets are used in the same objective function and one model is produced through the optimization process. The approach is based on the concept that each data set has a priority to constrain the inversion process at a specific part of the model.

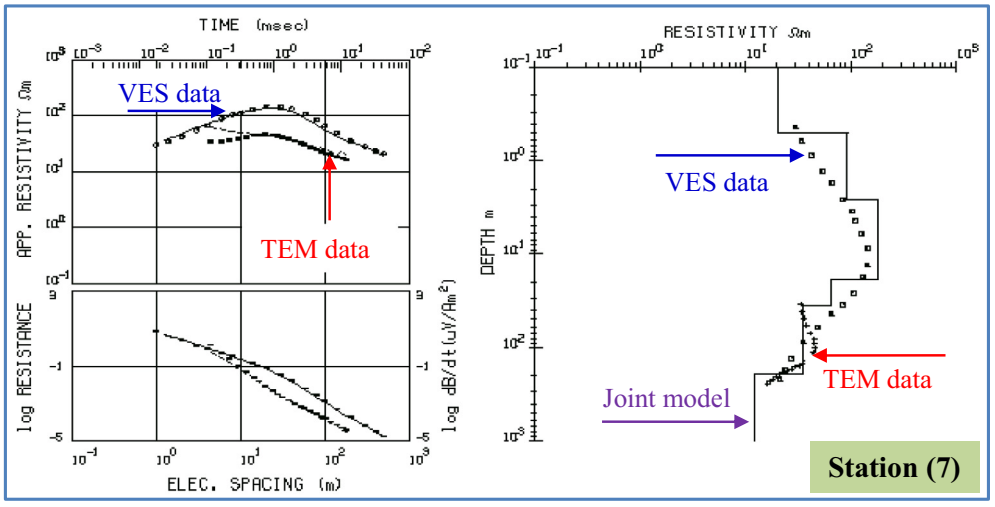

Figure 7a The model obtained from VES–TEM joint inversion at station No. 7 (rms: 3.1%).

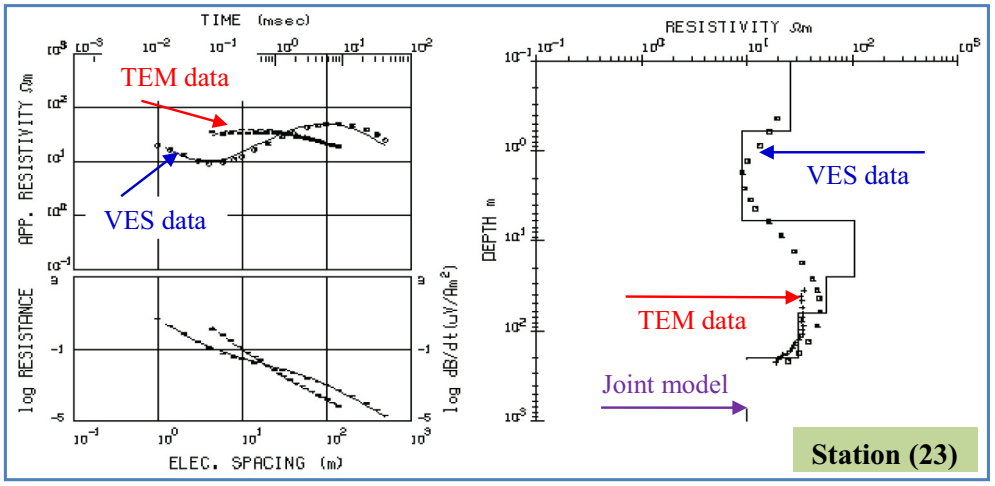

Figure 7b The model obtained from VES–TEM joint inversion at station No. 23 (rms: 2.2%).

In the present work, the VES and TEM curves were first analyzed using the scaling relationships (Meju, 2005) to determine the presence of any static shift in the DC data and check their suitability for joint inversion. The apparent resistivity curves do not exhibit substantial vertical shifts relative to the overlapping TEM curves. Besides, the VES sounding curves exhibit a reasonable degree of correlation with the TEM curves revealing that they are suitable for the joint inversion. The VES–TEM data have been jointly inverted in a 1-D scheme using the DCEMINT code (Meju, 2000). The final output of the joint inversion was a set of models; each of them describes the subsurface geoelectrical parameters at a specific measuring location. The rms misfit values are within the accepted range and they are ranging from 1.1% to 7.5% for the joint models. Fig. 7a and b shows two examples of sounding curves for the comparable VES and TEM data sets, and their best-fit joint models.

Inspection of Fig. 7a and b revealed the following features:

- The shallow part of the joint models is constrained only by the VES data; the middle part is controlled by both VES and TEM data sets, while the deeper part is mainly constrained by the TEM data.
- SIX geoelectrical layers could be identified from the joint inversion process at the majority of VES–TEM stations. The upper most three layers (1, 2 and 3) in the joint models are identical with their corresponding layers on the VES models. Then, the joint model response exhibits a best fitting with the observed resistivity values at the shallower parts of the sounding curves (up left side of Fig. 7a and b).
- The middle layers (4 and 5) of the joint models are obtained as a contribution of both VES and TEM data sets. They show some comparable differences in their parameters due to the different ground volumes sampled by the two methods.
- The last layer (6) of the joint model is determined mainly by the TEM data.

It is evident that the joint inversion shows significant advantages over the individual inversions the VES and TEM data sets. Therefore, the joint models have been considered as the final models used for the cconstruction of the geoelectrical and geological sections of the subsurface medium in the study area.

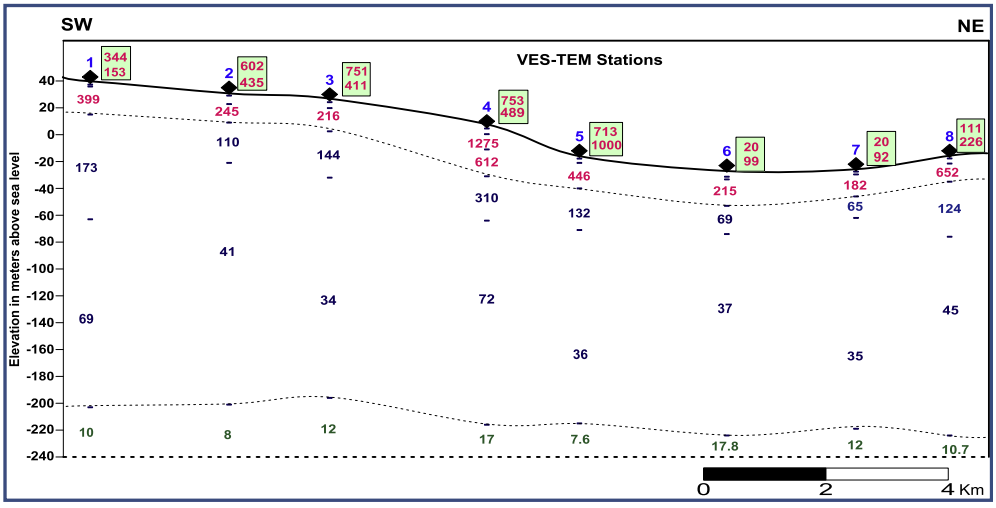

Figure 8 Geoelectrical cross-section along the line A–A′ (numbers in the frames above the section are the resistivity values of uppermost layers 1 and 2).

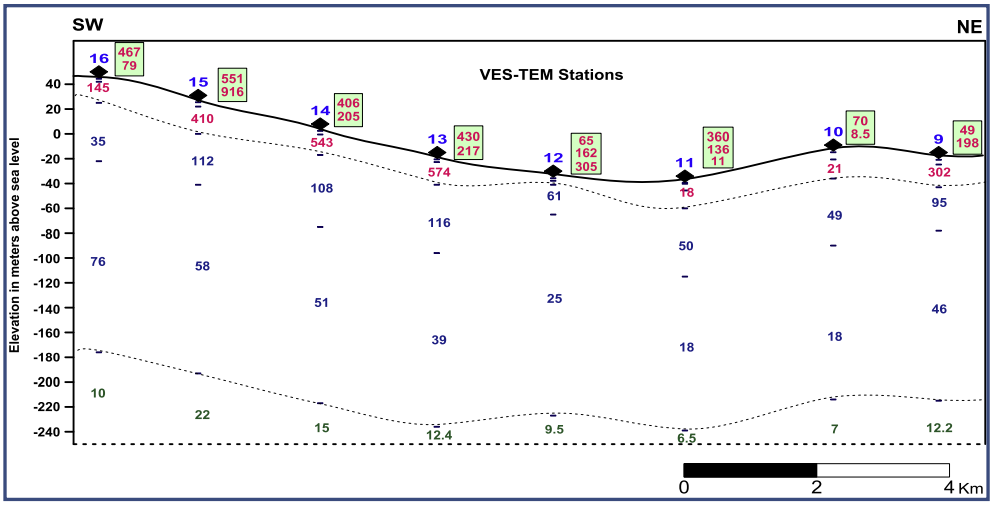

Figure 9 Geoelectrical cross-section along the line B–B′.

5. Cross sections

The VES–TEM joint models were used for the construction of THREE geoelectrical cross sections along the lines A–A′, B–B′ and C–C′ as shown in Fig. 5. Graphical displays of these sections are shown in Figs. 8–10.

Inspection of the cross-sections revealed that SIX geoelectrical layers have been identified in the investigated medium at the study area. These layers could be grouped in THREE composite units based on the available geologic information. The units are uniformly continuous and no structural features could be identified in the investigated section. The composite units can be described as follows:

- The first unit includes the upper-most three geoelectrical layers (1, 2 and 3), where these layers represent the surface and near surface medium. This unit (layers 1, 2, and 3) attains its minimum thickness of 6 m below station **12** and its maximum thickness of 36 m beneath station **4**. As a composite unit, it exhibits a mean resistivity values ranging from 18 Ohm-m to 720 Ohm-m, although some constituting layers show minimum resistivity less than 10 Ohm-m and maximum resistivity exceed 1000 Ohm-m. The wide resistivity range reflects the weathering conditions of the surface layer, dryness and wetness situations as some stations locate in the desert area and others in the cultivated land, and also could be attributed to the lithological variations.
- The second unit comprises the 4th and 5th geoelectrical layers. This unit represents the Pleistocene aquifer which is the main groundwater reservoir in the El Sadat area. This unit exhibits average resistivity values ranging from 27 to 115 Ohm-m with a relatively uniform thickness ranging from 171 m to 218 m. The Pleistocene aquifer consists of successive layers of sand and gravel intercalated with thin clay lenses.

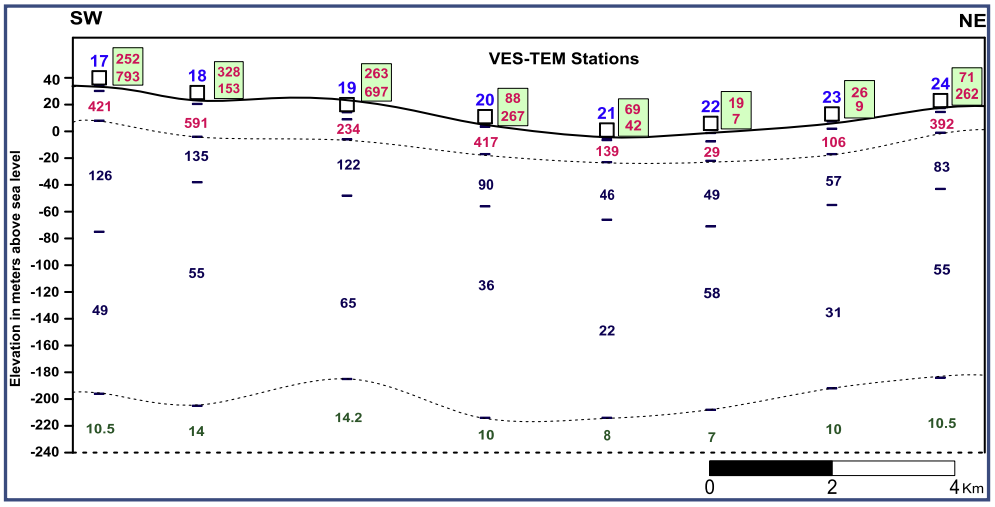

Figure 10 Geoelectrical cross-section along the line C–C′.

- The third unit is the last detected (6th) layer in the subsurface medium. This unit constitutes the base of the overlying Pleistocene aquifer. It shows low resistivity values ranging from 6.0 to 22 Ohm-m. The upper surface of this unit is reached at depth values ranging from 192 to 241 m from the ground surface, while the bottom of this unit could not be detected by the applied acquisition parameters. The third unit is composed mainly of sand and clay sediments of the Pliocene age (Menco, 1990 in Ahmed et al., 2011).

6. Water-bearing formations

From the geophysical study conducted at the El Sadat area and correlation with the hydrogeological information, TWO aquifer systems could be described; the shallow aquifer of Pleistocene age and the deeper aquifer of the Pliocene age.

6.1. Pleistocene aquifer

To evaluate this aquifer at the El Sadat area, the obtained geophysical models were used for the construction of FIVE contour maps describing spatial distribution of the geoelectrical properties and the estimated salinity values of this aquifer. These maps demonstrate the depth to the upper surface, thickness, resistivity distribution, transverse resistance and salinity distribution as shown in Fig. 11. Integrated interpretation of these maps assisted in better understanding of the present situation of the aquifer.

6.1.1. Depth to top surface

Generally, the Pleistocene aquifer is shallow and of semi-confined to un-confined character. The upper surface of this aquifer could be detected at depth values ranging from 6 to 36 m below the ground surface (Fig. 11a). It is noticed that aquifer is shallow at the northeastern part of the area (cultivated land), and is deeper in the southwestern desert area. This may be due to infiltration of excessive irrigation water to the aquifer leading to rising of the water table at this planted land.

6.1.2. Thickness of the aquifer

The aquifer is thick enough in the study area to be considered as a long-acting water resource as big thickness means high water content in this saturated sand-gravel aquifer. The aquifer attains it minimum thickness of 171 m at station No. 6 and maximum thickness of 218 m at station No. 1 (Fig. 11b).

6.1.3. Resistivity distribution

The Pleistocene aquifer exhibits moderate resistivity values ranging from 27 to 115 Ohm-m (Fig. 11c). Although the aquifer shows relatively low resistivity values at some locations around the oxidation ponds, the majority of resistivity values are in the moderate range (more than 50 Ohm-m). The moderate resistivity structure could indicate low to moderate salinity and in turn a good water quality. The low resistivity values obtained around the wastewater ponds may be attributed to increasing of clay content and/or saline water infiltrated from the ponds.

6.1.4. Transverse resistance

In addition to the two basic parameters, resistivity (ρ) and thickness (h) of the Pleistocene aquifer, two further parameters can be derived for this water-bearing layer. They are the *Longitudinal Conductance (S)* in mS and *Transverse Resistance (T)* in Ohm-m^2 where, $S = h/\rho$ and $T = h^*\rho$. S and T parameters bear more important relationships with hydrogeological information than do resistivity and thickness alone because using S and T, it is not necessary to use layer resistivity and layer thickness, thus giving rise to layer *equivalence*. In this concern, transverse resistance has been calculated for the Pleistocene layer from the relation: $T = h^*\rho$ at each measuring site. The obtained values are ranging from 4877 to 23108 Ohm-m^2 (Fig. 11d).

6.1.5. Salinity as estimated from electrical conductivity

Electrical conductivity (σ) of a solution is a measure of its ability to carry an electric current. Because the electrical conductivity and total salt concentration (TDS) of an aqueous solution are closely related, electrical conductivity is commonly used as an expression of the TDS concentration of an

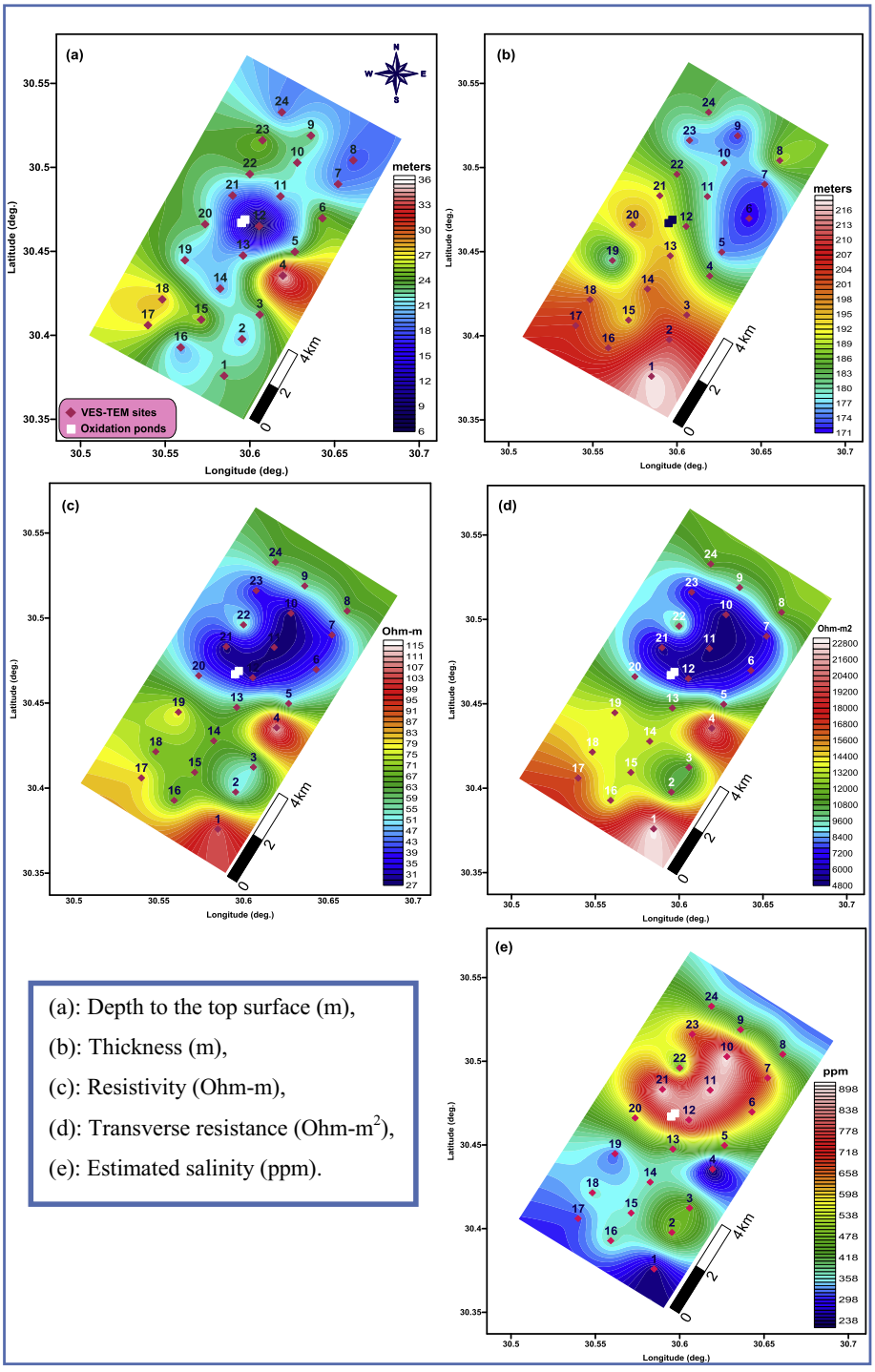

Figure 11 Contour maps show the distribution of geoelectrical parameters and the calculated salinity values in the Pleistocene aquifer.

aqueous sample. McNeill, 1990 proposed an approximate relationship between the bulk soil electrical conductivity and the ionic concentration of the soil solution.

$$\sigma_o(\mathrm{mS/m}) \approx \frac{1}{25} \times TDS\ (\mathrm{ppm})$$

where, σ_o is the bulk soil electrical conductivity (mS) and TDS is the total dissolved salts (ppm). This relation has been used to calculate the soil salinity of the Pleistocene aquifer at the study area and the results are displayed in Fig. 11e. The values of estimated soil salinity are ranging from 217 to 925 ppm.

6.2. *Pliocene aquifer*

The results obtained from this study are insufficient to provide a detailed description of the Pliocene aquifer at the study area. Just we could touch the upper surface of this aquifer at depths ranging from 192 to 241 m below the ground surface (Fig. 12a).

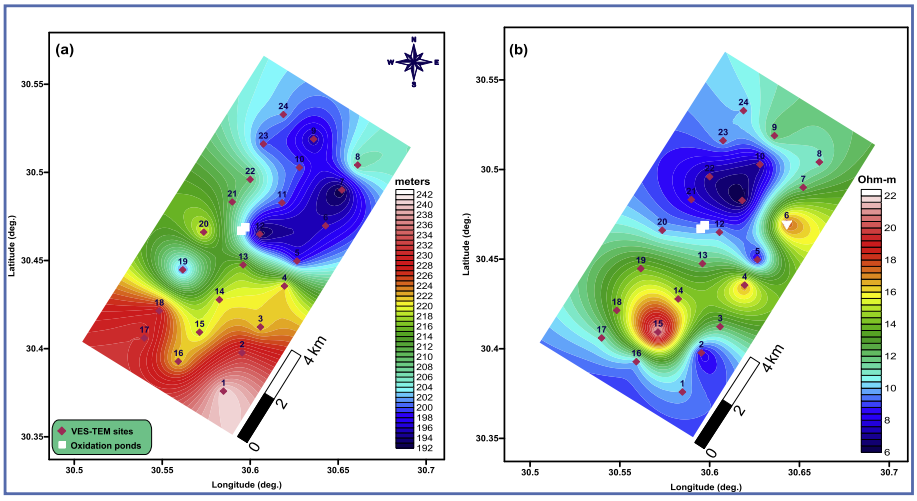

Figure 12 Contour maps show the (a) depth to the upper surface and (b) resistivity distribution of the Pliocene aquifer.

The aquifer is mainly composed of sandy clay sediments and it shows low resistivity values ranging from 6.0 to 22 Ohm-m (Fig. 12b). The groundwater of the Pliocene aquifer varies from fresh to brackish water. It is mainly fed by lateral seepage from the Delta and Moghra aquifers and also recharged from the south by the Nile Delta aquifer at Wadi El Farigh (Abdel Baki, 1983). In order to provide a full description for this aquifer, further investigations are required to fully understand its geological and hydrogeological situations.

Although, we could not provide a full picture of the Pliocene aquifer, detection of its top surface is very important as it acts as a marker bed defining the bottom of the main Pleistocene aquifer in this area.

7. Remarks and conclusion

- The VES and TEM are effective tools for groundwater studies and they are complementary to each other making them ideal partners for the joint inversion.
- The joint inversion is a powerful approach to overcome the problems of model equivalence, layer suppression, and to produce a well-constrained and robust multi-layer model for the subsurface medium.
- Multiple input parameters including VES and TEM data, geological and hydrogeological information have been utilized in this study. Moreover, different approaches including VES–TEM joint inversion, transverse resistance and salinity estimations have been applied and used for better description of the water-bearing formations at the study area.
- Inclusion of the transverse resistance was a big advantage used for detecting the most proper sites for new water wells. This is due to the direct relation between the transverse resistance and the hydraulic parameters of the aquifer. So, locations with high transverse resistance are expected to be of high transmissivity, where the latter is the ability of the aquifer to transmit water through the entire saturated thickness.
- TWO aquifer systems could be described in the study area; the Pleistocene and Pliocene aquifers. Pleistocene aquifer is the main one in this area and it received great interest in this study.
- The Pleistocene aquifer exhibits these parameters: depth to the upper surface is ranging from 6 to 36 m, the aquifer thickness is varying from 171 to 218 m, the resistivity is ranging from 27 to 115 Ohm-m, the transverse resistance is ranging from 4877 to 23,108 Ohm-m^2 and the salinity values are varying from 217 to 925 ppm.
- The low resistivity values shown around the oxidation ponds could be attributed to saline water infiltration from the ponds to the aquifer. Also, the shallower depth of the Pleistocene aquifer at the cultivated land might be due to surface infiltration from irrigation water and rising of the water level.
- The aquifer layer is continuous in the study area and no structural features corrupt this continuity.
- The proper locations for drilling new water wells that tap the Pleistocene aquifer are those that assure the following criteria: Higher resistivity (which means high water quality and/or low clay content), large saturated thickness (high water content), good water quality (low salinity), and lower depth values (low drilling cost).
- In the light of the fore-mentioned concept (the previous item) the water can be obtained from Pleistocene aquifer at all measuring stations with the following priorities:
- The **first** priority can be given to locations of the VES–TEM stations **1**, **4** and **17**, where these sites show the highest transverse resistance values (i.e., maximum resistivity and/or maximum thickness) and in the same time show minimum salinity.
- The **second** priority will be given to the site including stations **14**, **15**, **16**, **18** and **19**, where these locations show moderate transverse resistance and low salinity.
- The third priority is given to the sites including stations **2**, **3**, **5**, **8**, **9**, **13**, **20** and **24**, where these locations exhibit moderate transverse resistance and moderate salinity.
- The last preference will be given to the sites of stations **6**, **7**, **10**, **11**, **12**, **21**, **22** and **23**, where they show minimum transverse resistance and maximum salinity.
- The depth to the upper surface of the Pliocene aquifer is ranging from 192 to 241 m. It consists of sandy clay facies and shows low resistivity values ranging from 6 to 22 Ohm-m.

– Detection of the top surface of this sandy clay aquifer is a big advantage because it acts as a marker bed that defines the bottom of the main Pleistocene aquifer in this area.
– Further geophysical, hydrogeological and hydrochemical studies should be conducted to investigate the hydraulic parameters and water quality of the Pleistocene aquifer and to fully describe the deeper aquifer of the Pliocene Age.

References

Abdel Baki, A.A., 1983. Hydrogeological and hydrogeochemical studies on the area west of Rosetta branch and south of El Nasr canal (PhD Thesis). Fac Sci Ain Shams Univ, Cairo, Egypt, p. 156.

Abu Zeid, K., 1984. The geology of Wadi El Natrun, Western Desert, Egypt (M.Sc. Thesis). Cairo University.

Ahmed, M.A., Abdel Samie, S.G., El-Maghrabi, H.M., 2011. Recharge and contamination sources of shallow and deep groundwater of pleistocene aquifer in El-Sadat industrial city: isotope and hydrochemical approaches. Environ. Earth Sci. 62, 751–768.

Attia, S.H., 1975. Pedology and soil genesis of the quaternary deposits in the region west of the Nile Delta (Ph.D. Thesis). Faculty of Science, Ain Shams University, Cairo, p. 288.

Christensen, N.B., Sørensen, K.I., 1998. Surface and borehole electric and electromagnetic methods for hydrogeophysical investigations. Eur. J. Environ. Eng. Geophys. 3, 75–90.

Dawoud, M.A., Darwish, M.M., El-Kady, M.M., 2005. GIS-based groundwater management model for western Nile Delta. Water Resour. Manage. 19, 585–605.

Diab, M.Sh., Mahammed, M.A., Rizk, Z.S., 1995. The role of geology, hydrogeology and human activities in the contamination of shallow water resources northwest of the Rosetta Nile Branch, Egypt. J. Fac. Sci. United Arab Emirates Univ. 8 (2), 260–291.

El Shazly, E.M., Abdel Hady, M.A., El Ghawaby, M.A., El Kassas, I.A., El Khawasik, S.M., El Shazly, M.M., Sanad, S., 1975. Geological interpretation of Landsat satellite images for west Nile Delta area, Egypt. Remote Sensing Research Project, Academy of Scientific Research and Technology, Egypt, p. 86.

El-Abd, E., 2005. The Geological impact on the water bearing formations in the area south west Nile Delta, Egypt (Ph.D. Thesis). Geol. Depart. Fac. Sci., Menoufia Univ., p. 319.

El-Ghazawi, M.M., 1982. Geological studies of the Quaternary Neogene aquifers in the northwest Nile Delta (M.Sc. Thesis). Faculty of Science, Al-Azhar University, Cairo, Egypt, p. 170.

El-Kashouty, M., Sabbagh, A., 2011. Distribution and immobilization of heavy metals in Pliocene aquifer sediments in Wadi El Natrun depression, Western Desert. Arab. J. Geosci. 4 (5–6), 1019–1039.

Ghaly, S.S., 2001. Environmental impact of artificial recharge on groundwater in Bustan extension area (Master thesis). Faculty of Engineering-Ain Shams University, Egypt.

IPI2Win-1D Program, 2000. Programs set for 1D VES data interpretation, Dept. of Geophysics, Geological faculty, Moscow University, Russia.

Jupp, D.L.B., Vozoff, K., 1975. Joint inversion of geophysical data. Geophys. J. Roy. Astron. Soc. 42, 977–991.

Khalil, M.A., Abbas, A.M., Santos, F., Massoud, U., Salah, H., 2013. Application of VES and TDEM techniques to investigate sea water intrusion in Sidi Abdel Rahman area, northwestern coast of Egypt. Arab. J. Geosci. 6, 3093–3101.

Massoud, U., El Qady, G., Metwaly, M., Santos, F., 2009. Delineation of shallow subsurface structure by azimuthal resistivity sounding and joint inversion of VES–TEM data: case study near Lake Qaroun, El Fayoum, Egypt. Pure Appl. Geophys. 166 (2009), 701–719.

Massoud, U., Santos, F., El Qady, G., Atya, M., Soliman, M., 2010. Identification of the shallow subsurface succession and investigation of the seawater invasion to the Quaternary aquifer at the northern part of El Qaa plain, Southern Sinai, Egypt by transient electromagnetic data. Geophys. Prospect. 58, 267–277.

McNeill, J.D., 1990. Use of electromagnetic methods for groundwater studies. In: Ward, S.H. (Ed.) Geotechnical and Environmental Geophysics, SEG. Review and Tutorial, 1, 191–218.

Meju, M.A., 2000. DCEMINT code, a user-friendly multi-purpose system for DC and TEM forward modeling and inversion. Max. A. Meju, Dept. of Environmental Science, Lancaster University, Lancaster LA1 4YQ, U.K.

Meju, M.A., 2005. Simple relative space–time scaling of electrical and electromagnetic depth sounding arrays: implications for electrical static shift removal and joint DC-TEM data inversion with the most-squares criterion. Geophys. Prospect. 53, 463–479.

Menco, 1990. Misr company for engineering and agricultural projects report.

Metwaly, M., Elawadi, E., Moustafa, S.S.R., Al-Arifi, N., 2014. Combined inversion of electrical resistivity and transient electromagnetic soundings for mapping groundwater contamination plumes in Al Quwy'yia Area, Saudi Arabia. JEEG 19 (1), 45–52.

Raiche, A.P., Jupp, D.L.B., Rutter, H., Vozoff, K., 1985. The joint use of coincident loop transient electromagnetic and Schlumberger sounding to resolve layered structures. Geophysics 50, 1618–1627.

RIGW, 2002. Evaluation of different uses for the groundwater in Sadat City. Technical Report No. 3, Research Institute for Groundwater.

RIGW and IWACO, 1990. Vulnerability of groundwater to pollution in the Nile Valley and Delta, El Kanater El Khairia, Egypt TN 70.130-89-02.

RIGW and IWACO, 1991. Monitoring and control groundwater pollution in the Nile Delta and adjacent desert areas, El Kanater El Khairia, Egypt, TN 77.01300-91-12.

Said, R., 1962. The Geology of Egypt. Elsevier Publisher, Amsterdam and New York.

Saleh, M.F., 1980. Some hydrogeological and hydrochemical studies on the Nile Delta (M. Sc. Thesis). Faculty of Science, Ain Shams University, Cairo, Egypt.

Sandberg, S.K., 1993. Examples of resolution improvement in geoelectrical soundings applied to groundwater investigations. Geophys. Prospect. 41 (8), 207–227.

Shata, A.A., 1953. New light on the structural development of the western desert of Egypt. Bull. Desert Res. Inst. Egypt 3 (1), 101–106.

Shata, A.A., 1955. An introductory note on the geology of the northern period of the western desert of Egypt. Bull. Desert Res. Inst. Egypt 5 (3), 96–106.

TEMIX XL 4, 1996. Temix xl V. 4 user's manual, Interpex. Colorado, USA, p. 468.

The World Bank, 2007. West Delta water conservation and irrigation rehabilitation project. Report No. 32393-EG.

Wassef, R., 2011. Development of a groundwater flow model for water resources management at the development area west of the rosetta branch, Egypt (PhD thesis) Faculty of Natural Sciences, Martin Luther University, Halle-Wittenberg, Germany.